

## Article

# Hydrothermal Carbonization Process of Digestate from Sewage Sludge: Chemical and Physical Properties of Hydrochar in Terms of Energy Application

Małgorzata Wilk <sup>1,\*</sup>, Marcin Gajek <sup>2</sup>, Maciej Śliz <sup>1</sup>, Klaudia Czerwińska <sup>1</sup> and Lidia Lombardi <sup>3</sup>

<sup>1</sup> Department of Heat Engineering and Environment Protection, AGH University of Science and Technology, Mickiewicza 30 Av., 30-059 Kraków, Poland

<sup>2</sup> Faculty of Materials Science and Ceramics, AGH University of Science and Technology, Mickiewicza 30 Av., 30-059 Kraków, Poland

<sup>3</sup> Niccolò Cusano University, Via don Carlo Gnocchi 3, 00166 Rome, Italy

\* Correspondence: mwilk@agh.edu.pl

**Abstract:** Hydrochars (HTCD) derived from digestates, namely D1 and D2 (from two plants) of sewage sludge, were examined with respect to their fuel properties. The hydrothermal carbonization (HTC) tests were performed at temperatures of 200 and 220 °C, for 2 and 4 h of residence times, and with 1:10 and 1:8 digestate to water ratios (D/W), causing an increase of ash content (max. 55.8%), and a decrease c.a. 20% of the higher heating value except for a slight increase to 15 kJ/kg at 200 °C and 4 h in hydrochars. Conversely, the combustion profiles of hydrochars moved towards higher temperatures (225–257 °C) and finished earlier at lower temperatures (423–438 °C). The HTCD from D1 and D2 showed very similar properties under the same conditions (200 °C, 4 h, 1:8 D/W) for combustion characteristic temperatures, indices and profiles. The best efficiency was found for HTCD2. In addition, the polluted post-processing liquid phase was treated by a distillation process providing 30% higher pH, 50% lower BOD values, up to 15 times lower COD values, and c.a. three times lower conductivity.

**Keywords:** hydrothermal carbonization; sewage sludge; hydrochar; digestate; thermal analysis; post-processing water



**Citation:** Wilk, M.; Gajek, M.; Śliz, M.; Czerwińska, K.; Lombardi, L. Hydrothermal Carbonization Process of Digestate from Sewage Sludge: Chemical and Physical Properties of Hydrochar in Terms of Energy Application. *Energies* **2022**, *15*, 6499. <https://doi.org/10.3390/en15186499>

Academic Editor: Andrea De Pascale

Received: 13 August 2022

Accepted: 2 September 2022

Published: 6 September 2022

**Publisher's Note:** MDPI stays neutral with regard to jurisdictional claims in published maps and institutional affiliations.



**Copyright:** © 2022 by the authors. Licensee MDPI, Basel, Switzerland. This article is an open access article distributed under the terms and conditions of the Creative Commons Attribution (CC BY) license (<https://creativecommons.org/licenses/by/4.0/>).

## 1. Introduction

Every sector that utilizes biomass generates biodegradable waste, which can then be transformed via different methods, is primarily for energy production. One method is anaerobic digestion, considered to be the best biological transformer of organic waste [1], employing the help of microbes, and resulting in the production of biogas [2]. Organic and municipal wastewater waste can be successfully utilized in biogas plants producing biogas as the main product and digestate as a by-product. Anaerobic digestion involves a sequence of reactions such as hydrolysis, acidogenesis and methanogenesis [3]. Digestate is a substance which is rich in nutrients and contains both organic and inorganic compounds as well as micro-organisms. Due to a significant amount of organic matter in the digestate, it can be used as a solid biofuel, a soil amendment or a substrate for activated carbon production. Most of the digestate (c.a. 95%) produced in Europe is used as fertilizer, but some impurities (e.g., biological and heavy metals), and law regulations can limit this utilization, such as European Nitrates Directive (91/676/EEC) [4]. There are a few disadvantages linked with the anaerobic digestion process. The digestates are often significantly diluted (commonly from 3 to 6% dry mass), have a colloidal structure responsible for significant problems with their mechanical dewaterability, and contain inorganic impurities, including alkali and/or heavy metal compounds. They are characterized by a low calorific value of dry matter (organic compounds contained in the substrates for biogas plants have already

been mostly converted into biogas in the process of methane fermentation) and they create strong odours. If the digestate cannot be used for field fertilization due to exceeding the permissible content of contaminants, additional methods concerning utilization have to be found.

The digested sewage sludge still contains a large quantity of non-biodegradable organic matter that can be used for additional energy production. The most common usage of digested sewage sludge is drying combined with combustion, but the high moisture content in a feedstock is cost consuming [5]. Effective energy management may be improved by a suitable pretreatment to help solve this problem. In fact, a high amount of moisture in the digestate makes hydrothermal carbonization, treatment or conditioning, the most adequate method. Additionally, a part of the biogas could be used for its energy demand. Moreover, the hydrothermal conditioning of sewage sludge significantly improves its dewaterability, which may help with a reduction of heat consumption in all processes, in accordance with the European key objectives action plan, by focusing on “waste-to-energy” in the circular economy and, thereby, increasing waste prevention, reuse and recycling.

Hydrothermal carbonization (HTC) is a thermochemical process which involves the application of heat and pressure to convert the digestate in the presence of water into a solid product, namely hydrothermally carbonized material or hydrochar. The process is generally carried out within a temperature range of 180–350 °C, and the pressure is maintained above saturation pressure to ensure the liquid state of water. Additionally, the residence time is maintained between one and several hours. Under those rigid conditions, the chemical destruction of the dry mass of feedstock occurs and the following reactions take place: hydrolysis, decarboxylation, and dehydration [6]. This results in three types of products: gases, mainly CO<sub>2</sub>, water and some simple organic compounds dissolved in water. A solid product, (30–40% moisture content), can be easily filtered from the reaction solution, and has upgraded carbon-like physical and chemical properties (e.g., hydrophobic, non-biodegradable). The liquid phase, which is often a major product, may be highly toxic, reaching relatively high values of chemical oxygen demand (COD) including up to 45 gO<sub>2</sub>/L in the case of sewage sludge used as feedstock and, hence, requires proper management. The efficiency of the process depends chiefly on the physical and chemical structure of feedstock, reaction temperature, reaction time, pressure and pH. The main advantage of this pretreatment method is to increase the dewaterability (drying) of the obtained hydrochar with respect to the feedstock, which is five times less energy-consuming than drying. The researchers attracted a great deal of attention for the HTC process, because it is energy-efficient, simple and low cost. Moreover, the energy required to heat the reacting water is very low in comparison with traditional thermochemical processes. As previously mentioned, the process is specific to biomass with a high moisture content, and mainly includes municipal waste, e.g., sewage sludge [6,7]; food factory waste, e.g., beetroot, citrus, orange, herbal tea, pulp mill waste, olive mill, wine industry or tobacco stalks [8–13]; agricultural waste, e.g., straw, lignocellulosic or algae biomass [14–18], and also digestate from biogas plants [19]. The physical and chemical properties of the hydrochar and its yield depend primarily on the properties of the feedstock and the processing conditions (temperature and residence time), which is why research on their impact is required for every studied feedstock. Moreover, during hydrothermal carbonization, the morphology changes significantly with temperature from macroporous to micro carbonaceous spheres on the surface, mainly caused by dehydration and decarboxylation of polymers followed by aromatization and re-condensation reactions [20], resulting in hydrophilic heterogeneous structures of hydrochar. In general, during the biomass degradation under hydrothermal carbonization, the inorganic elements are released and dissolved in the processing solution; thus, a lower ash content is found in hydrochar than in raw biomass [21]. In the case of sewage sludge, the opposite results have been found [22]. Due to the excess loss of volatile matter and retention of minerals, an increase of ash in hydrochar is observed. The HTC also modifies the porous structure and surface area of sewage sludge, but high temperatures and long residence times are not desirable as they cause limited porosity and a small surface

area. However, according to Wang [22], the abundant oxygen-containing functional groups on its surface indicate the potential for good adsorptive properties for heavy metals, and xenobiotic organism retention. Sewage sludge was also studied by Tasca et al. [23], who reviewed the hydrochar properties towards different applications, namely: energy sector, soil amelioration, wastewater pollution remediation, and carbon and greenhouse gases sequestration. In addition, the methods for treatment of the post-processing liquid phase were also analyzed. Furthermore, the fate of heavy metals was also investigated since sewage sludge is considered as an extremely complicated heterogeneous material that contains organic debris, inorganic particles, bacteria, colloid sewage sludge and moisture, as well as undesirable components, such as heavy metals, organic pollutants and pathogens, which are environmentally hazardous [24–27]. The hydrothermal treatment of sewage sludge has been investigated, taking into account the possible application of hydrochars as adsorbents, land fertilizer or renewable fuel [28–30]. However, the contents of heavy metals seriously limit their application. The reported research suggests that changing HTC process parameters (e.g., temperature, time, catalyst, and the addition of other biomass) could influence the total contents and chemical forms of heavy metals [31], mainly with an increase of temperature in the process. The significant impact of feedstock properties has created a wide range of investigations resulting in many documented studies concerning a variety of feedstock, primarily in renewable energy generation. Sharma et al. [32] reviewed the waste biomass and its conversion by using the conventionally heated HTC process, modified by microwave assistance, and confirmed the advantages of hydrothermal carbonization of waste biomass towards renewable energy generation potential. Although there have been many investigations concerning the hydrothermal carbonization of sewage sludge [33,34], fewer studies have considered the hydrothermal carbonization process of its digestate [35–38]. Aragón-Briceño et al. [39] investigated the process temperature on the characteristics of hydrochars including the fate of nitrogen and phosphorus species in energy application. The post-processing liquid phase from the hydrothermal process in terms of the biochemical methane potential was also tested. Both hydrochar and the post-processing liquid phase were found to have some potential for use in additional energy production. The same idea was investigated by Parmar and Ross [40], who studied the HTC of four different digestates from disparate origins: agricultural residue, sewage sludge, residual municipal solid waste, and vegetable, garden, and fruit waste. It appeared that the hydrothermal carbonization process enhanced biogas production, but the solid product, due to a high ash content, was not recommended as a fuel. It was indicated that hydrochar should be studied further in terms of utilization as a soil amender.

Cao et al. [41] investigated the fundamentals of the effect of digestate origin and process conditions. Although many researchers are interested in the hydrothermal treatment of digestate and are enthusiastic about this idea, they underline that not only the conditions of the process, but also the feedstock origin and its properties highly influence the resulting products and their properties. Composition and chemical energy can vary even between the same types of digestate depending on the source [6,9,19,39–43]. Moreover, discussion of the optimal conditions at a lower range of temperatures for producing hydrochar with homogeneous and constant fuel properties derived from digestate of sewage sludge is crucial from an industrial point of view to provide clear guidance for the design, optimization and economy of the HTC process when hydrochar is dedicated to energy application. The use of a higher range of temperature and pressure requires higher capital and operating costs of the HTC installation and more complex procedures concerning technical inspection. Therefore, further research on process conditions and properties of feedstock is still required to discover the overall benefits from hydrothermal processes as a post-treatment step after the anaerobic digestion of sewage sludge.

Accordingly, the main goal of this study was to investigate the hydrothermal carbonization process of digestate under different conditions of the HTC process. The novelty of this work is a comparative analysis of physical and chemical properties of hydrochars and liquid phases derived from the hydrothermal carbonization of digestates from two

different sewage treatment plants. Therefore, the fuel characteristics as well as the thermal combustion behaviour (TGA), including combustibility indices and kinetic analyses of solid hydrochars, were investigated and compared to feedstock. Following-up the preliminary, less developed study of the distillation of post-processing water from sewage sludge, previously presented by the authors [6], where it was highlighted it as a very promising approach, further analyses were carried out. The liquid phase was analyzed in terms of its physical properties, and possible disposal, and application in, for example., biogas production or liquid biofertilizer. For these reasons, the following indicators were characterized according to standard analytical methods for Chemical Oxygen Demand, Biochemical Oxygen demand, conductivity, pH and acidity. The results could provide a better understanding of the hydrothermal conversion of the digestate of sewage sludge in order to successfully optimize this pre-treatment process and give a multifaceted description of digestate and its hydrothermally carbonized products.

## 2. Materials and Methods

### 2.1. Materials

Two filtrated, dewatered, aerobically stabilized types of sewage sludge were investigated. Both were collected from municipal sewage treatment plants at the same time of the year: in the summer. The first (D1) was taken from Płaszów, a metropolitan area of Kraków, (c.a. 780,000 inhabitants), Poland. The second (D2) was taken from the Silesian industrial district area of Gliwice, (c.a. 184,000 inhabitants), Poland, where wastewater was collected. Both digestates were stored, briefly in the refrigerator at 4 °C prior to the experiments. Samples from both materials were air dried, pulverized, and then stored in sealed containers before further comparative tests. The moisture content in the raw digestates were determined: for D1 it was 76.25%, whereas, in the case of D2, it was 80%. Both materials were diluted with deionized water for hydrothermal carbonization tests.

### 2.2. Hydrothermal Carbonization Test

The hydrothermal carbonization tests were performed using a stainless steel Zipperclave<sup>®</sup> Stirred Reactor equipped with a built-in stirrer produced by Parker Autoclave Engineers, Hessinger Dr, Erie, PA, USA. The full procedure was presented by Wilk [44]. Briefly, the diluted material D1 at either 1:8 or 1:11 digestate to water ratio was introduced to the reactor. The isolated reactor was heated up to 200 °C or 220 °C and maintained for a residence time of 4 h. In the case of D2, material was diluted at a 1:8 digestate to water ratio, and two residence times, 2 and 4 h, and a temperature of 200 °C were applied. Finally, the heat was turned off and the main reactor was cooled down by cooling water to room temperature. The solution was evacuated from the reactor and was filtrated through microfiltration paper using the ceramic Buchner funnel vacuum filtration setup. Both products, solid and liquid, were weighed before further testing was undertaken. The solid product was oven dried at 105 °C for 24 h and then pulverized prior to physical and chemical analyses. The liquid product was immediately investigated to avoid any changes in its properties. The hydrothermally carbonized samples were named according to the method used and the feedstock number, namely HTCD1 and HTCD2, which corresponded to digestates D1 and D2, and then were numbered according to the applied conditions.

### 2.3. Methods for Analysis of Solid Materials

The ultimate analysis was performed using the Elemental Analyser Leco 628, according to PKN-ISO/TS 12902:2007. The proximate analysis including moisture, ash and volatile content were determined under the following standards, PN EN ISO 18134-2:2017, PN EN ISO 18122:2016, and PN EN ISO 18123:2016, respectively. The higher heating values were determined using a KL-10 bomb calorimeter, according to PN-ISO 1928:2002. Mass and energy yields of hydrochars were determined according to [45].

### 2.3.1. Combustion Performance and Behaviour

The TGA analysis, in an air atmosphere ( $40 \text{ mL min}^{-1}$ ), and at a heating rate of 10, 20, and  $30 \text{ K}\cdot\text{min}^{-1}$  using the Netzsch STA 449 F3 Jupiter apparatus, was performed. The samples (10 mg) were heated in alumina crucibles (capacity  $70 \mu\text{L}$ ) from an ambient temperature up to  $700 \text{ }^\circ\text{C}$ . Based on TG and DTG results, performed at a heating rate of  $10 \text{ K min}^{-1}$ , the combustion characteristic temperatures including  $T_i$ —the ignition temperature,  $T_{\text{max}}$ —maximum peak temperature, and  $T_b$ —burnout temperature, were determined. The ignition ( $D_i$ ), burnout ( $D_f$ ), combustion stability ( $H_f$ ) and comprehensive combustion (S) indices were also calculated to evaluate the combustion performance [34].

### 2.3.2. Kinetic Analysis

Three isoconversion methods: Friedman, Kissinger-Akahira-Sunose and Flynn\_Wall\_Ozawa, were employed to estimate the most significant factor of kinetics: the activation energy. These methods were adopted due to their reliability and currency by other researchers [46]. The activation energy was determined by measuring the temperatures corresponding to fixed values of  $\alpha$  from experiments at different heating rates from the slope of a plot of  $\ln\beta$  vs.  $1/T$ , where  $\alpha$  was a conversion rate for the sample

$$\alpha = \frac{m_{i0} - m_a}{m_{i0} - m_f} \quad (1)$$

and  $m_{i0}$ ,  $m_a$ , and  $m_f$  were the initial mass of the sample, the actual mass, and mass after combustion in g. The ratio of solid-state reaction rate was described by the following equation, where  $t$  and  $T$  were the time and temperature of the process, respectively, and  $k$  the rate constant:

$$\frac{d\alpha}{dt} = k(T)f(\alpha) \quad (2)$$

A number of approximation formulas and different methods were applied to calculate the activation energy. The Friedman method was based on the following equation:

$$\ln\left[\beta \frac{d\alpha}{dT}\right] = \ln[A_\alpha f(\alpha)] - \frac{E_{a\alpha}}{RT_\alpha} \quad (3)$$

The Kissinger-Akahira-Sunose method was expressed by

$$\ln\left(\frac{\beta}{T_\alpha^2}\right) = \ln\left(\frac{A_\alpha R}{E_{a\alpha} g(\alpha)}\right) - \frac{E_{a\alpha}}{RT_\alpha} \quad (4)$$

The Flynn-Wall-Ozawa method was based on:

$$\ln \beta = \ln\left[\frac{0.0048E_a}{Rg(\alpha)}\right] - 1.0516 \frac{E_a}{RT} \quad (5)$$

### 2.3.3. Structural Analysis

Scanning electron microscopy supported by energy dispersive spectroscopy was investigated by an FEI Inspect S50 microscope. Additionally, Fourier Transformation Infrared Spectroscopy was performed by Bruker spectroscope, which investigated the wavelengths of studied samples in the range  $400\text{--}4000 \text{ cm}^{-1}$ . Both methods were used to determine changes in the structure and surface of the digestates and their hydrothermally carbonized samples [9].

## 2.4. Methods for Analysis Methods of the Liquid Phase

The liquid phase, derived from the filtration process after the hydrothermal carbonization test, was non-translucent and of a dark colour; thus, the distillation process, performed under low pressure, was applied for purification [6]. For both the liquid phase and its distillate, the following analyses were conducted: chemical oxygen demand (COD) analysis,

according to PN-ISO 6060:2006, and pH, conductivity, and biological oxygen demands (BOD) were measured by the Multifunction Laboratory Meter CX-505 ELMETRON in order to make a comparative analysis. Additionally, an acid-base titration of the distillate was carried out to determine the concentration of acetic acid. All measurements were repeated at least three times. The remaining dark solid part from the distillation process was dried at 105 °C, weighed and then analysed, using the Elemental Analyser Truespec Leco 628 according to PKN-ISO/TS 12902:2007, for its carbon content to determine the carbon balance.

### 3. Results and Discussion

The results of ultimate and proximate analyses supported by higher and lower heating values (HHV and LHV) are summarized in Table 1.

**Table 1.** Characteristics of feedstocks and hydrothermally carbonized digestates, db.

	D1	HTCD1_1	HTCD1_2	HTCD1_3	HTCD1_4	D2	HTCD2_1	HTCD2_2
Temperature, °C		200	200	220	220		200	200
Digestate to water ratio		1:8	1:11	1:8	1:11		1:8	1:8
Residence time		4	4	4	4		2	4
Ultimate analysis								
C, %	29.6	26.2	26.50	26.70	26.00	32.8	30.4	30.8
H, %	4.3	3.14	3.34	3.14	3.05	4.69	3.83	3.84
N, %	4.35	2.32	2.14	2.16	1.95	4.74	2.55	2.52
S, %	1.58	1.42	1.32	1.36	1.51	1.61	1.43	1.55
O, %	20.11	11.12	12.34	9.44	11.21	22.85	12.67	11.93
Proximate analysis								
FC, %	8.16	9.01	10.45	10.96	11.88	8.66	9.42	9.24
VM, %	50.45	34.03	33.08	31.18	30.58	53.83	39.59	39.46
Ash, %	40.06	55.80	54.36	57.20	56.28	33.31	49.12	49.36
M, %	1.33	1.16	2.11	0.66	1.26	4.20	1.89	1.94
Fuel ratio								
FC/VM	0.16	0.26	0.32	0.35	0.39	0.16	0.24	0.23
Heating values								
HHV, MJ/kg	14.34	11.40	11.40	13.41	11.41	14.66	13.76	15.12
LHV, MJ/kg	13.57	10.82	11.45	12.73	10.80	13.75	13.09	14.46

The chemical changes in the properties of all hydrothermally carbonized digestates were compared to raw materials and depicted in a van Krevelen diagram visualized in Figure 1. Due to the decarboxylation, dehydration and demethanation reactions, which occurred in the aqueous environment under temperature and pressure, the molar ratios of O/C and H/C were much lower in comparison with the raw materials. Consequently, they moved into a more coal-like zone towards the lower end of the scheme. Organoleptic analysis confirmed that all hydrothermally carbonized materials were more carbonaceous, brittle and easier to grind than raw dried digestates. Regarding both raw materials, the digestates derived from sewage sludge of different origins, and the ultimate and proximate analysis indicated that they were similar from a chemical and physical point of view. Carbon and volatile matter contents were slightly higher in D2 when compared to D1, whereas ash content, conversely, was lower. The changes in the chemical properties of the samples presented in Figure 1 clearly indicated that the temperature and digestate to water ratio had an impact on the properties of hydrothermally treated material; the HTCD1\_3 samples derived at 220 °C and a digestate to water ratio of 1:8, moved significantly to the left side of the scheme than the other wet torrefied samples from D2. A similar tendency was observed regarding the increased residence time of the process: HTCD2\_2 at 4 h also moved to the more carbonaceous zone. These results are consistent with those presented by

He et al. [47]. Even though the higher temperature was applied to produce HTCD1\_3, the location of this sample was closer to HTCD2\_2, which was produced at a lower temperature but with the same residence time and digestate to water ratio. This is due to the slightly higher carbon content in D2 and its hydrothermally carbonized samples.

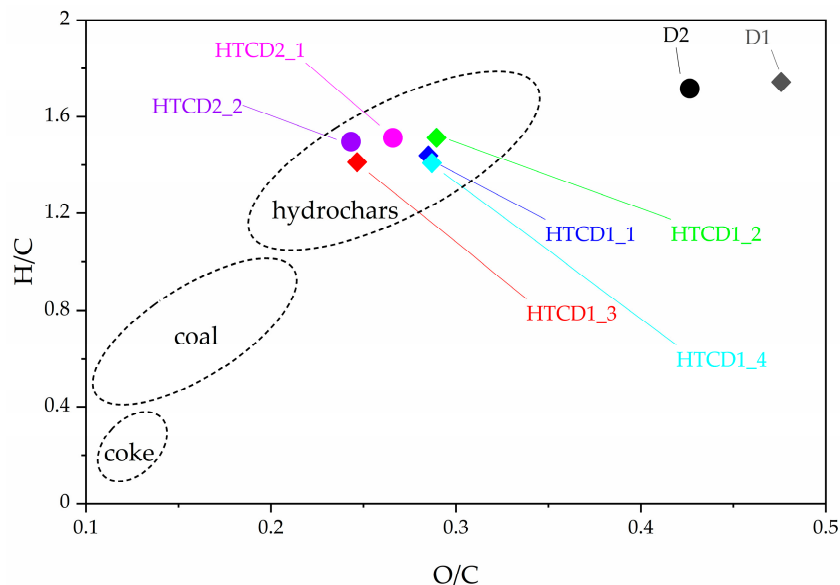


**Figure 1.** Van Krevelen diagram.

The fuel ratio (FC/VM) grades the hydrochars as an alternative carbonaceous fuel [41]. Since for HTCD1 the values of FC increased and VM decreased with dilution of feedstock for the HTC process and carbonization temperature, the fuel ratio increased from 0.16 to 0.39. In the case of HTCD2, the fuel ratio also increased by about 50% due to an increase of FC and a decrease of VM caused by the HTC process. However, the increase of carbonization time from 2 to 4 h did not affect the fuel ratio, which is contrary to the results of He et al. [47].

The ultimate analysis also indicated changes in the nitrogen and sulphur contents caused by the HTC process. The significant removal of nitrogen content from digestates was observed due to the degradation of proteins containing N which occurs above 150 °C, and decomposition of organic-N to NH<sub>4</sub>-N [7]. The higher dilution (1:11) and higher temperature (220 °C) applied in the HTC of D1 resulted in 50 and 55% of N release into gases and liquid phases. In the case of D2, the increase of reaction time was not significant and the removal of N was 46% for both HTCD2\_1 and HTCD2\_2. Regarding sulphur, the HTC process caused a slight removal, but increased dilution and temperature did not indicate a clear tendency. The increase of carbonization time caused an increase of sulphur in the hydrochar, which is consistent with Aragón-Briceño et al. [39]. In conclusion, the NO<sub>x</sub> and SO<sub>x</sub> emissions from the combustion of hydrochars will be lower than in the case of digestates derived from sewage sludge, proving that hydrochar is the more favourable fuel. The physical properties are presented in Figure 2. The mass yields for HTCD1 differ between 52 and 64%, which is related to the applied conditions. The highest value of 64% was obtained for HTCD1\_1 performed at 200 °C and a digestate to water ratio of 1:8, whereas the lowest was for HTCD1\_2 performed at 200 °C and a digestate to water ratio of 1:11. Energy yields were almost the same for samples studied in different digestate to water ratios, and the temperature impact on these properties was not visible. The fixed carbon increased slightly with an increase in temperature, which corresponded to a decrease in volatile matter content in the samples. The more diluted material and higher temperature of the process, the less volatile matter and higher fixed carbon in the samples were found. In the case of HTCD2, the highest mass yield was found in the sample conducted for 4 h of residence time, and fixed carbon, found for 2 h of residence time, which was lower than for

4 h, where it was slightly higher than in the case of D2. When comparing hydrothermally carbonized samples derived under the same conditions, namely 200 °C of temperature, digestate to water ratio of 1:8 and 4 h of residence time, the mass yield of HTCD1\_1 was slightly higher and differed by only 3% from HTCD2\_2. However, energy yields were lower, around 23% when compared with HTCD2\_2, indicating that this material reacted differently despite being under the same conditions of the process. Higher heating values were depicted for all samples, confirming the above statement. In the case of D1, the hydrothermal treatment caused a decrease in HHV, whereas with D2, there was a slight increase. The results were similar to those presented by [35].

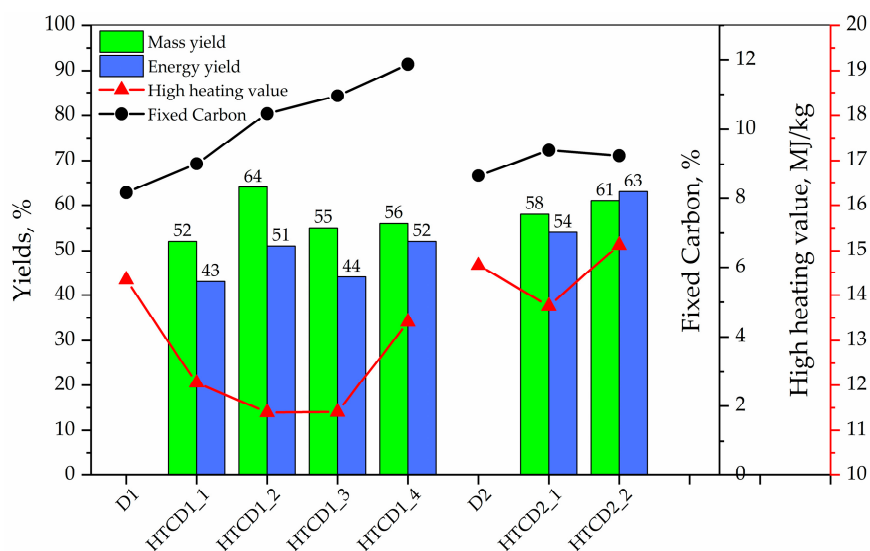


**Figure 2.** Chemical and physical properties.

Thermal analysis was conducted in order to study the combustion profiles of the samples. The results were depicted in the forms of TG/DTG/DSC curves (Figures 3a and 4a) for D1 and D2. The combustion process was observed on TG profiles. It was divided into three distinct stages: release of the moisture content, release and combustion of volatile matters, and, finally, combustion of the char. A lack of changes in the mass of solid residue indicated the end of the process. The combustion of the two raw digestates was similar. However, the TG curves were the same in shape and character; D2 initiated the combustion slightly later and combusted longer at a higher temperature (504 °C) for 3 min when compared to D1 (488 °C). The combustion process was much more visible with DTG curves, which occurred with two peaks: one c.a. 270 °C, and, more noticeably, the second highest weight loss was observed around 480 °C. The char combustion was confirmed by the DSC peak, which corresponded with the second DTG peak.

The comparison between TG curves of hydrothermally carbonized products derived from D1 and D2 are presented in Figures 3b and 4b. The TG profiles of carbonized samples differed and moved slightly towards higher temperatures. In both cases, a sharp decrease was observed between 250–300 °C and a much higher quantity of solid residue was collected after the treatment. Concerning HTCD1 samples, the TG profiles of HTCD1\_1 and HTCD1\_2 differed when compared to HTCD1\_3 and HTCD1\_4. Both HTCD1\_1 and HTCD1\_2, showed greater decreases and higher rates of volatile matter release represented by DTG1 curves. The location of DTG1 for HTCD1\_2 suggested that its volatile matter was more violently combusted at a lower temperature, 272 °C, than in the case of HTCD1\_1, namely 280 °C. The other two samples, HTCD1\_3 and HTCD1\_4, derived at a higher temperature, 220 °C, initiated and finalized the combustion at the same moment, and also combusted with two peaks of DTG, but with less intensity as in the case of the previously mentioned HTCD1\_1 and HTCD1\_2.

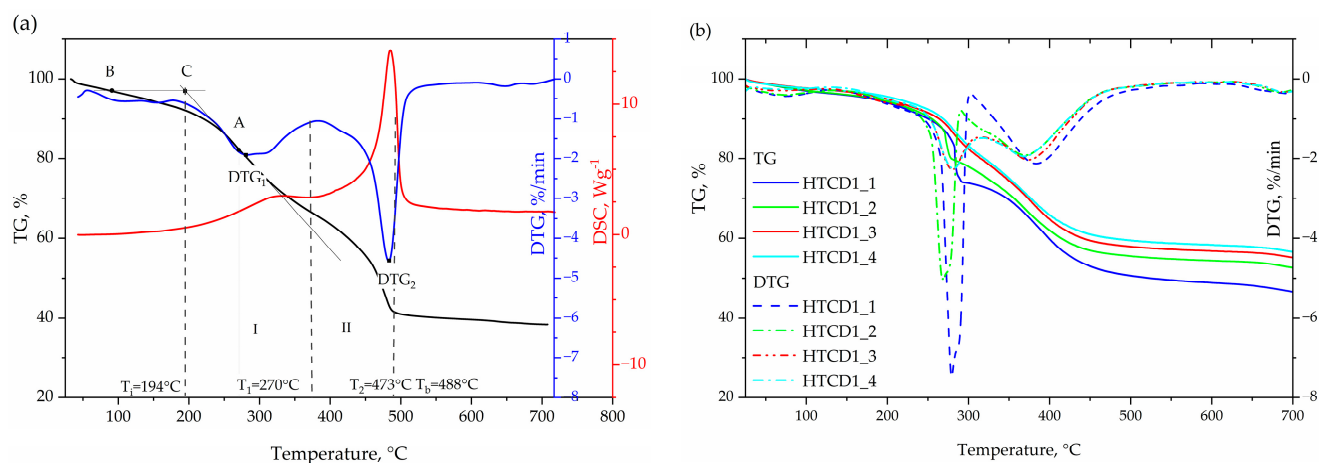


Figure 3. (a) TG/DTG/DSC of D1 and (b) TG curves of HTCD1.

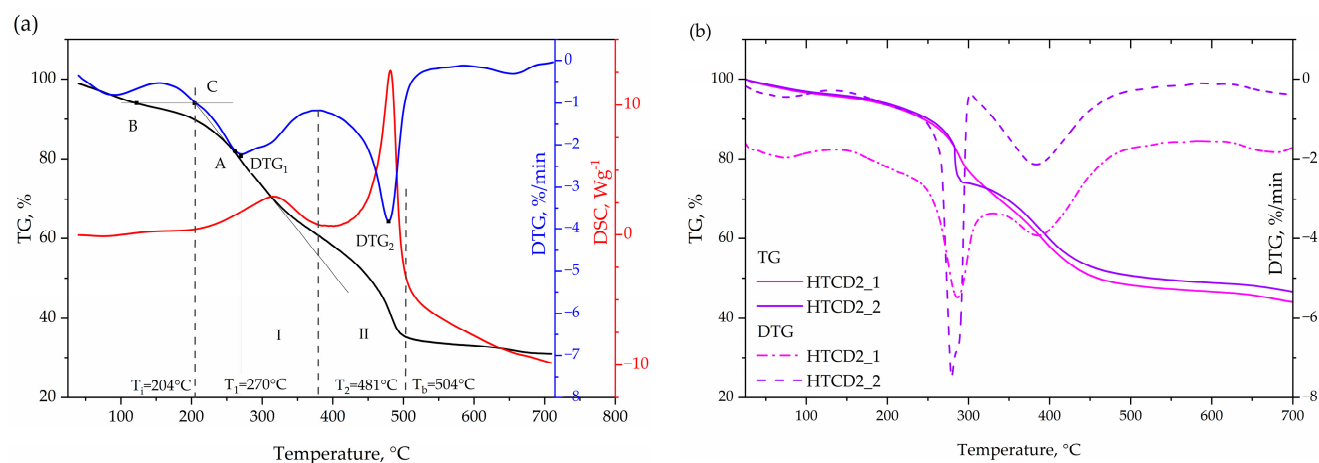


Figure 4. (a) TG/DTG/DSC of D2 and (b) TG curves of HTCD2.

In addition, based on the TGA results, the most important combustion parameters including characteristic temperatures and combustibility indexes, were determined and summarized in Table 2. The following temperatures were found:  $T_i$ —ignition temperature, which defined the beginning of the combustion,  $T_1$ —was the maximum peak temperature, and  $T_b$ —burnout temperature indicated the temperature at which the fuel was completely combusted [47]. In both cases, the hydrothermal carbonization caused the shift of  $T_i$  temperatures in HTCD1 and HTCD2 samples towards higher temperatures, due to an intensive volatile release confirmed by  $D_i$ . The  $T_b$  occurred earlier in the case of pretreated samples, indicating that they were combusted in a shorter time, and according to a higher value of  $S$  index, with a higher intensity and probably more easily due to a slightly better combustion performance. The  $H_f$  represents the rate and intensity of the combustion process. Additionally, the results proved that the hydrothermally carbonized process unified the properties of the pretreated samples conducted under the same conditions giving very similar values of combustion characteristic temperatures, indexes and profiles for HTCD1\_1 and HTCD2\_2. For instance, the ignition indexes ( $D_i$ ) were 1.41 and 1.34 ( $\%/(\text{min}^3)$ ), respectively. The comprehensive combustion ( $S$ ) index differed only by 1.7 ( $\%/(\text{min} \cdot \text{K}^2)$ ) and combustion stability ( $H_f$ ) index by 5 ( $\%/(\text{min}^2 \cdot \text{K}^3)$ ). A higher temperature of the process (220 °C) caused a decrease in  $S$ , providing results approximately half lower (c.a.  $S = 6.5$  ( $\%/(\text{min} \cdot \text{K}^2)$ )) and an increase of about 40–50 in the  $H_f$  value. In conclusion, according to Song et al. [48] the results indicated that hydrochars from digestates performed better ignition and combustion characteristics in comparison to both digestates due to a larger  $D_i$  index and a higher value of the  $S$  index.

**Table 2.** The combustion characteristics parameters of raw and hydrothermally carbonized digestates.

Material	D1	HTCD1_1	HTCD1_2	HTCD1_3	HTCD1_4	D2	HTCD2_1	HTCD2_2
Temperature, °C		200	200	220	220		200	200
Digestate to water ratio		1:8	1:11	1:8	1:11		1:8	1:8
Residence time		4	4	4	4		2	4
$T_i$ , °C	194	250	255	225	225	204	250	257
$T_b$ , °C	488	438	423	427	423	504	442	438
$T_1$ , °C	270	280	272	280	282	270	290	280
$DTG_1$ , %/min	−4.00	−7.67	−5	−2.27	−2.25	−2.72	−4.58	−7.46
$T_2$ , °C	473	384	363	374	370	481	384	382
$DTG_2$ , %/min	−5.50	−2.54	−2.36	−2.02	−1.94	−5.29	−2.54	−2.16
$D_i$ , %/min <sup>3</sup> ·10 <sup>−2</sup>	0.63	1.41	0.94	0.48	0.47	0.66	0.82	1.34
$D_b$ , %/min <sup>4</sup> ·10 <sup>−5</sup>	9.5	30.9	22.4	9.3	10.3	12.3	18.0	30.9
$S$ , % <sup>2</sup> /(min <sup>2</sup> ·°C <sup>3</sup> )·10 <sup>−8</sup>	11.7	21.1	12.1	6.6	6.4	12.4	12.9	19.4
$H_f$ , %/(min·°C <sup>2</sup> )	875	972	973	1026	1014	813	992	967

The activation energy was estimated by three isoconversional model-free methods, Friedman, Kissinger-Akahira-Sunose, and Flynn-Wall-Ozawa [49] for D1 and D2 and their pretreated samples derived under the same conditions, 200 °C, 4 h of residence time and 1:8 of digestate to water ratio, namely HTCD1\_1 and HTCD2\_2 (Table 3). An example for  $E_a$  determination is presented in Figure 5, where the Kissinger-Akahira-Sunose model was used. Different heating rates ( $\beta = 10, 20, 30$  K/min) were applied and the slope of  $\ln(\beta/T_2)$  for different conversion rates ( $\alpha$ ) was depicted. For the evaluation, only the fittings with a high correlation coefficient were considered. Raw samples of D1 and D2 showed nearly parallel fittings for most of the conversion rates, indicating that activation energy changes slightly with ongoing combustion. HTCD samples display a greater variation, suggesting a multistep kinetic mechanism [50,51]. All methods provided very similar results, especially in the case of D2 and its hydrothermally carbonized product, which differed by only 1 to 12%. The activation energy for raw D1 was lower, c.a 30%, when compared to pretreated material, and this was probably the result of the degradation of organic compounds in sewage sludge.

**Table 3.** Activation energy estimated by Friedman, Kissinger-Akahira-Sunose and Flynn-Wall-Ozawa.

Material	$E_a$ , kJ/kmol		
	Friedman	Kissinger-Akahira-Sunose	Flynn-Wall-Ozawa
D1	132	179	152
HTCD1	169	180	182
D2	165	166	153
HTCD2	168	169	152

FTIR spectra of D1 and D2 digestates and their hydrochars HTCD1 and HTCD2 are depicted in Figure 6a,b. There were no significant changes found in the digestates after hydrothermal treatment, indicating that the hydrothermal carbonization process slightly affected the chemical bond of digestates, which corresponds with Peng's investigations [52]. Both digestates were similar in shape, but the intensity of peaks differed a little. For instance, with D2 the peak at 3400 cm<sup>−1</sup>, which is attributed to the vibration of -OH stretching found in cellulose, decreased slightly with a rise in temperature and dilution, suggesting the ability for dehydration, whereas, in the case of D1, it was weaker for a shorter period of the hydrothermal carbonization process. The wavelength range of 2800–3000 cm<sup>−1</sup> is assigned to aliphatic hydrocarbons, most likely aliphatic carbon C-H and the symmetrical stretching of methylene groups, represented by 2923 and 2853 cm<sup>−1</sup>, respectively [53], which were slightly affected by temperature and time of the process. Two peaks found in the region of

1350–1800  $\text{cm}^{-1}$  at 1658 and 1442  $\text{cm}^{-1}$  were probably attributed to the stretching vibration of C=N amides [52,54] and the presence of olefins components [55]. In both studied cases they were slightly weaker after hydrothermal conditioning. The strong and broad peak at 1007 (D1) or 1011  $\text{cm}^{-1}$  (D2) is connected to -C-OH, attributed to carboxylic acids or alcohols. The other hypothesis is that these peaks are assigned to Si-O stretching and Si-O-Si bonds, confirming the presence of Si in digestates from sewage sludge. According to Wang et al. [56], polysaccharides can be detected in the region of 1000–1100  $\text{cm}^{-1}$  after decomposition caused by the hydrothermal carbonization process. There are also some subtle peaks below the region 600–400  $\text{cm}^{-1}$  slightly affected by the hydrothermal process, which are probably caused by Si-O or Al-O bending vibration [47].

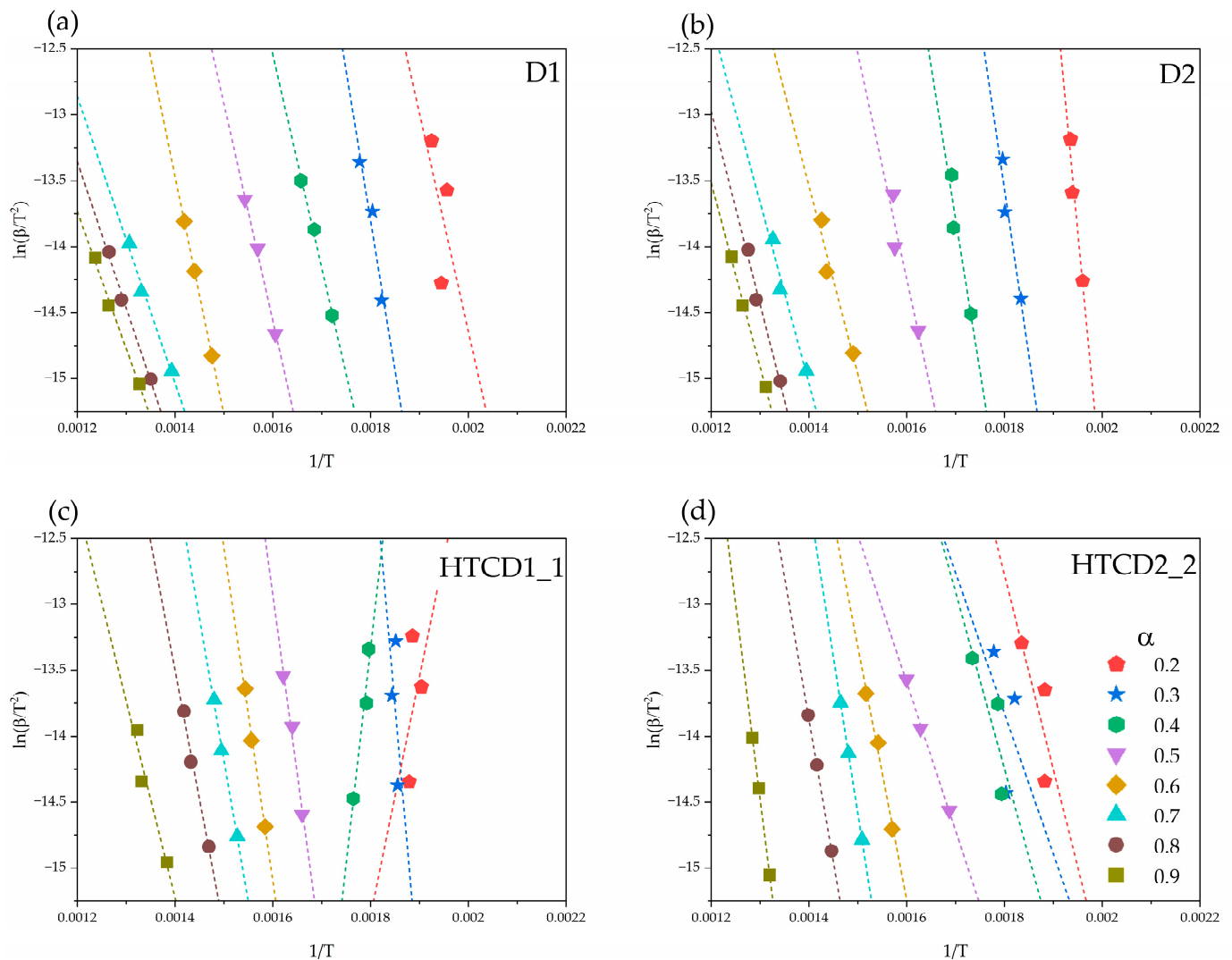


**Figure 5.** Linear fitting to the Kissinger-Akahira-Sunose kinetic model for various conversion during combustion for: (a) raw D1, (b) raw D2, (c) HTCD1\_1, and (d) HTCD2\_2.

SEM-EDS results depicted in Figures 7 and 8 confirmed the degradation observed by FTIR analysis caused by the hydrothermal carbonization process of pretreated digestates. In both cases defragmentation was also found, and smaller particles were observed after the process.

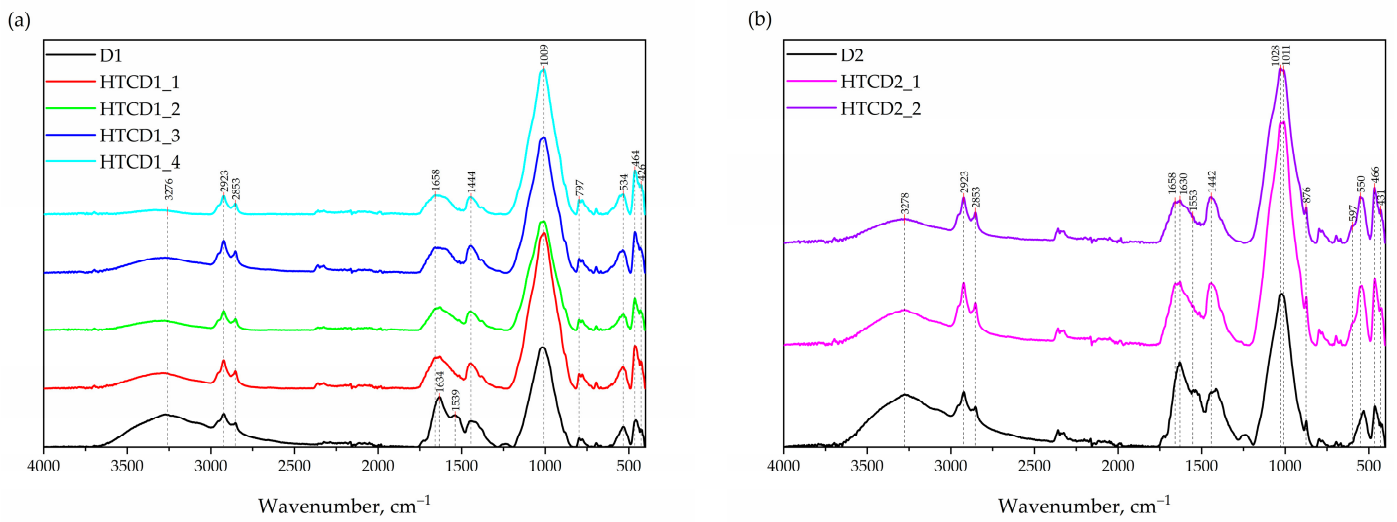


Figure 6. FTIR results for (a) D1 and HTCD1 and (b) D2 and HTCD2.

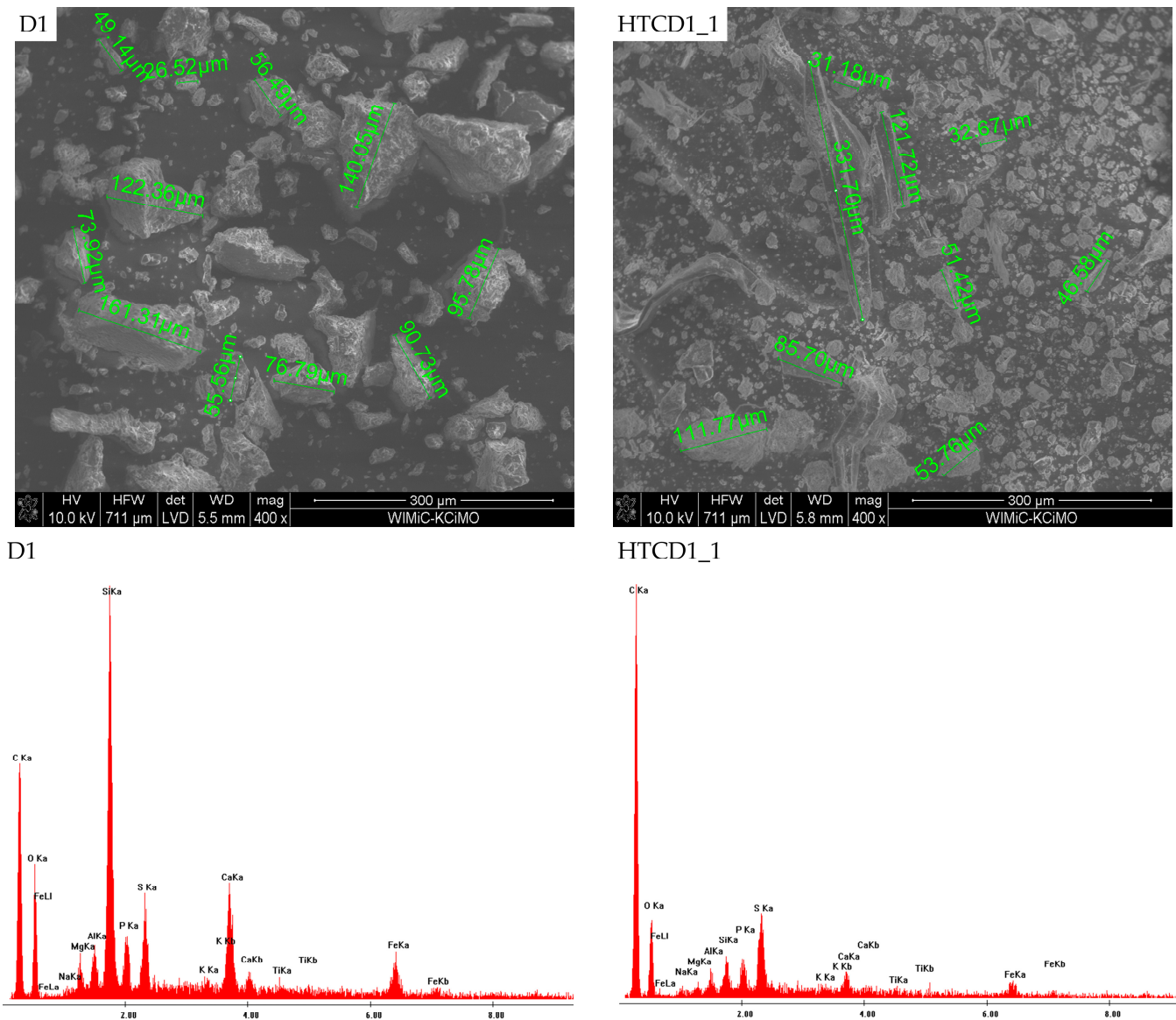


Figure 7. SEM-EDS results for D1 and HTCD1\_1.

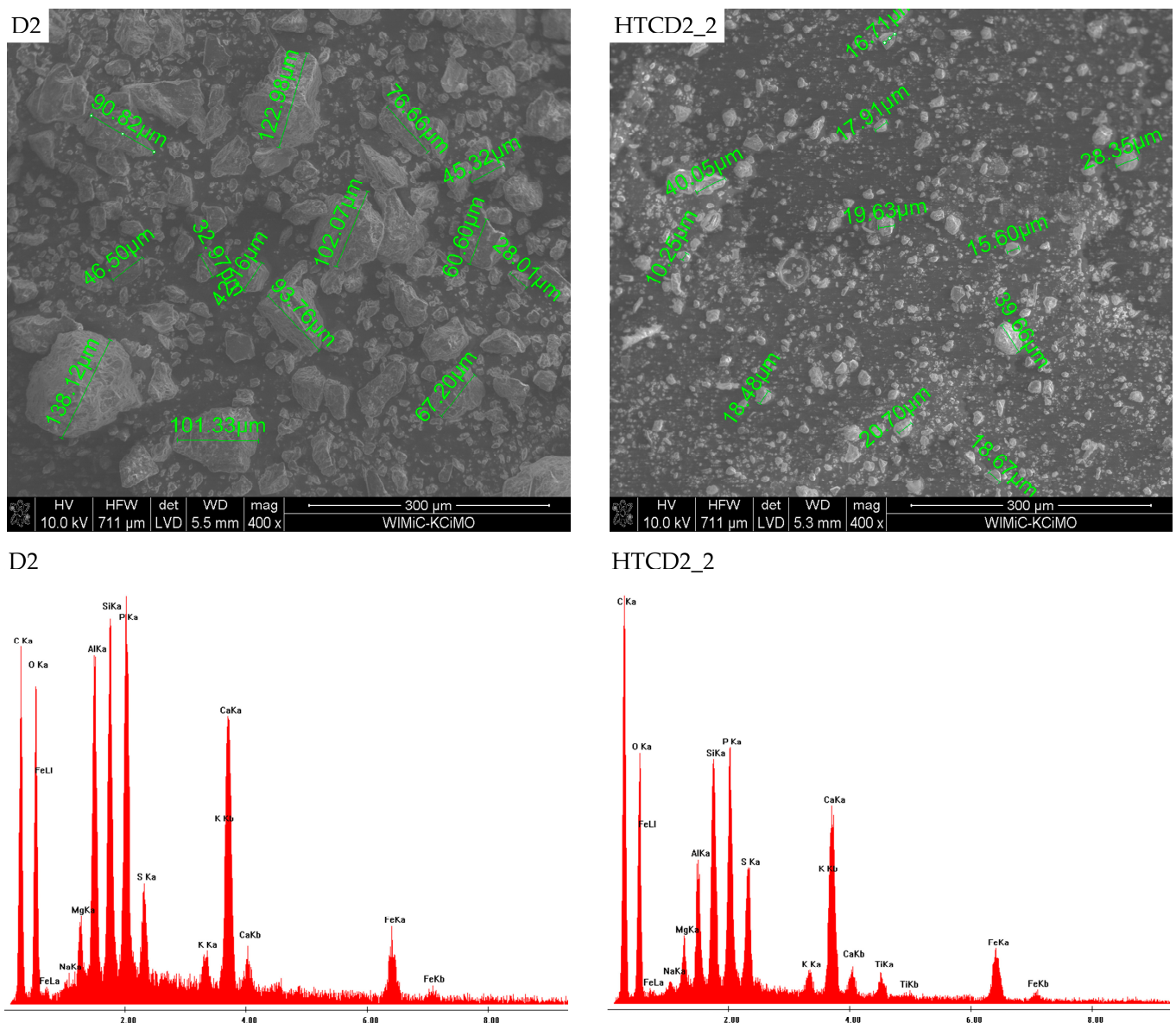


Figure 8. SEM-EDS results for D2 and HTCD2\_2.

Liquid contains a high quantity of dissolved total organic carbon content and nutrients and necessitates adequate disposal. Accordingly, the preliminary study of vacuum distillation of the post-processing liquid phase was tested as a suitable method for purification. This method proved to be a good solution, not only for the elimination of odour and colour from non-translucent and toxic liquid, but also as an effective method in COD, BOD and conductivity reduction [6]. Table 4 summarized the results presenting that COD was decreased by ten times, BOD by two times and conductivity by four times, even though pH increased by 30%.

**Table 4.** Liquid filtrate and its distillate characteristics.

Material	HTCD1_1	HTCD1_2	HTCD1_3	HTCD1_4	HTCD2_1	HTCD2_2
pH	7.33	7.00	7.74	7.46	7.09	7.13
pH <sub>d</sub>	9.5	9.18	8.87	8.95	9.09	8.94
Conductivity, mS	13.95	10.36	16.84	12.89	11.27	12.68
Conductivity <sub>d</sub> , mS	3.09	2.28	8.88	7.09	3.85	5.20
COD, gO <sub>2</sub> L <sup>-1</sup>	30.3	22.62	29.67	23.85	28.72	26.76
COD <sub>d</sub> , gO <sub>2</sub> L <sup>-1</sup>	3.16	1.49	4.57	3.33	2.77	2.37
BOD, gO <sub>2</sub> L <sup>-1</sup>	1.76	1.04	1.32	1.52	1.08	1.12
BOD <sub>d</sub> , gO <sub>2</sub> L <sup>-1</sup>	0.8	0.72	0.72	0.84	0.60	0.48

d—distillate.

#### 4. Conclusions

The digestates from two wastewater treatment plants were hydrothermally carbonized at 200 and 220 °C, 2 and 4 h of time, and 1:8 and 1:11 of D/W ratios. The changes in the physical and chemical properties of hydrochars were confirmed by proximate and ultimate analysis, thermal analysis and FTIR and SEM-EDS methods. Hydrothermal carbonization caused an increase of up to 50% of ash content and a decrease c.a. 6–12% of carbon content, which corresponded to a decrease c.a. 20% of the higher heating value except for a slight increase to 15 kJ/kg at 200 °C and 4 h in hydrochars. The degradation of morphology and structure caused by rigid conditions were confirmed by FTIR and SEM-EDS analysis. Energy and mass yields varied 52 to 64 and 43 to 63%, respectively. Thermal analysis presented combustion profiles of hydrochars which moved towards higher temperatures (225–257 °C) and finished earlier at lower temperatures (423–438 °C) in comparison to digestates. An important guidance for industry regarding the energy application of digestate from sewage sludge is provided. Indeed, one of the most significant aspects of the results is that the hydrochar properties are mainly dependent on the process conditions (200 °C, 4 h, and 1:8 D/W) rather than on the feedstock characteristics. This is very promising from an industrial point of view, because a single carbonization plant can process feedstock arriving from different waste water treatment plants, providing an homogenous and constant product output. In particular, the following properties were found to be unified for the two digestates: fixed carbon (c.a. 9.12%), combustion characteristic temperatures ( $T_i$  c.a. 254 °C,  $T_b = 438$  °C,  $T_1 = 280$  °C), indices ( $D_i$  c.a.  $1.37 \text{ min}^2 \cdot \text{C}^3 \cdot 10^{-2}$ ,  $D_b = 30.9 \text{ min}^2 \cdot \text{C}^3 \cdot 10^{-2}$ ,  $S$  c.a.  $20.25\% \text{ 2}/(\text{min}^2 \cdot \text{C}^3) \cdot 10^{-8}$ ,  $H_f$  c.a.  $970 \text{ min}^2 \cdot \text{C}^2$ ) and  $E_a = 169 \text{ kJ} \cdot \text{kmol}^{-1}$  calculated by the Friedman method. Moreover, to manage the problem of polluted process water, the vacuum distillation process is proposed as a successful disposal of the liquid phase from the hydrothermal carbonization process, thereby giving a spectacular reduction in the main toxicity indicators (two times lower BOD values, up to fifteen times lower COD values, and c.a. three times lower conductivity).

**Author Contributions:** Conceptualization, M.W.; data curation, M.W., M.G., M.Ś.; formal analysis, M.W., M.G., M.Ś., K.C. and L.L.; resources, M.W.; methodology, M.W., M.G., M.Ś.; investigation, M.W., M.G., M.Ś. and K.C.; funding acquisition, M.W., project administration, M.W., validation, M.W., M.G. and M.Ś.; visualization, M.W., M.G. and M.Ś.; supervision, M.W.; writing—original draft, M.W.; writing review & editing, M.W. and L.L. All authors have read and agreed to the published version of the manuscript.

**Funding:** This research was funded by the programme „Excellence initiative—research university” for the AGH University of Science and Technology, Poland [grant no 501.696.7995].

**Institutional Review Board Statement:** Not applicable.

**Informed Consent Statement:** Not applicable.

**Data Availability Statement:** Not applicable.

**Acknowledgments:** The authors would like to express their thanks to the proprietor of the experimental apparatus EKOPROD Ltd. in Bytom. The authors also wish to thank Józef Marszałek for his exceptional experimental help.

**Conflicts of Interest:** The authors declare that they have no conflict of interest. The funders had no role in the design of the study; in the collection, analyses, or interpretation of data; in the writing of the manuscript; or in the decision to publish the results.

## References

1. Lee, M.; Hidaka, T.; Hagiwara, W.; Tsuno, H. Comparative performance and microbial diversity of hyperthermophilic and thermophilic co-digestion of kitchen garbage and excess sludge. *Bioresour. Technol.* **2009**, *100*, 578–585. [[CrossRef](#)] [[PubMed](#)]
2. Lastella, G.; Testa, C.; Cornacchia, G.; Notornicola, M.; Voltasio, F.; Sharma, V.K. Anaerobic digestion of semi-solid organic waste: Biogas production and its purification. *Energy Convers. Manag.* **2002**, *43*, 63–75. [[CrossRef](#)]
3. Themelis, N.J.; Ulloa, P.A. Methane generation in landfills. *Renew. Energy* **2007**, *32*, 1243–1257. [[CrossRef](#)]
4. Dahlin, J.; Herbes, C.; Nelles, M. Biogas digestate marketing: Qualitative insights into the supply side. *Resour. Conserv. Recycl.* **2015**, *104*, 152–161. [[CrossRef](#)]
5. Werle, S. Sewage sludge-to-energy management in Eastern Europe: A Polish Perspective. *Ecol. Chem. Eng. S* **2015**, *22*, 459–469. [[CrossRef](#)]
6. Wilk, M.; Magdziarz, A.; Jayaraman, K.; Szymańska-Chargot, M.; Gökalp, I. Hydrothermal carbonization characteristics of sewage sludge and lignocellulosic biomass. A Comparative Study. *Biomass Bioenergy* **2019**, *120*, 166–175. [[CrossRef](#)]
7. Djandja, O.S.; Duan, P.G.; Yin, L.X.; Wang, Z.C.; Duo, J. A Novel machine learning-based approach for prediction of nitrogen content in hydrochar from hydrothermal carbonization of sewage sludge. *Energy* **2021**, *232*, 121010. [[CrossRef](#)]
8. Wilk, M.; Śliz, M.; Gajek, M. The Effects of hydrothermal carbonization operating parameters on high-value hydrochar derived from beet pulp. *Renew. Energy* **2021**, *177*, 216–228. [[CrossRef](#)]
9. Basso, D.; Patuzzi, F.; Castello, D.; Baratieri, M.; Rada, E.C.; Weiss-Hortala, E.; Fiori, L. Agro-industrial waste to solid biofuel through hydrothermal carbonization. *Waste Manag.* **2016**, *47*, 114–121. [[CrossRef](#)]
10. Pham, T.P.T.; Kaushik, R.; Parshetti, G.K.; Mahmood, R.; Balasubramanian, R. Food waste-to-energy conversion technologies: Current status and future directions. *Waste Manag.* **2015**, *38*, 399–408. [[CrossRef](#)]
11. Volpe, M.; Fiori, L. From olive waste to solid biofuel through hydrothermal carbonisation: The role of temperature and solid load on secondary char formation and hydrochar energy properties. *J. Anal. Appl. Pyrolysis* **2017**, *124*, 63–72. [[CrossRef](#)]
12. Saqib, N.U.; Sharma, H.B.; Baroutian, S.; Dubey, B.; Sarmah, A.K. Valorisation of food waste via hydrothermal carbonisation and techno-economic feasibility assessment. *Sci. Total Environ.* **2019**, *690*, 261–276. [[CrossRef](#)] [[PubMed](#)]
13. González-Arias, J.; Gómez, X.; González-Castaño, M.; Sánchez, M.E.; Rosas, J.G.; Cara-Jiménez, J. Insights into the product quality and energy requirements for solid biofuel production: A comparison of hydrothermal carbonization, pyrolysis and torrefaction of olive tree pruning. *Energy* **2022**, *238*, 122022. [[CrossRef](#)]
14. Wilk, M.; Magdziarz, A.; Kalemba-Rec, I.; Szymańska-Chargot, M. Upgrading of green waste into carbon-rich solid biofuel by hydrothermal carbonization: The effect of process parameters on hydrochar derived from acacia. *Energy* **2020**, *202*, 117717. [[CrossRef](#)]
15. Yuan, C.; Wang, S.; Qian, L.; Barati, B.; Gong, X.; Abomohra, A.E.; Wang, X.; Esakkimuthu, S.; Hu, Y.; Liu, L. Effect of cosolvent and addition of catalyst (HZSM-5) on hydrothermal liquefaction of macroalgae. *Int. J. Energy Res.* **2019**, *43*, 4843. [[CrossRef](#)]
16. Krylova, A.Y.; Zaitchenko, V.M. Hydrothermal carbonization of biomass: A review. *Solid Fuel Chem.* **2018**, *52*, 91–103. [[CrossRef](#)]
17. Zhou, S.; Liang, H.; Han, L.; Huang, G.; Yang, Z. The influence of manure feedstock, slow pyrolysis, and hydrothermal temperature on manure thermochemical and combustion properties. *Waste Manag.* **2019**, *88*, 85–95. [[CrossRef](#)]
18. Lee, J.; Lee, K.; Sohn, D.; Kim, Y.M.; Park, K.Y. Hydrothermal carbonization of lipid extracted algae for hydrochar production and feasibility of using hydrochar as a solid fuel. *Energy* **2018**, *153*, 913–920. [[CrossRef](#)]
19. Pawlak-Kruczek, H.; Niedzwiecki, L.; Sieradzka, M.; Mlonka-Mędrala, A.; Baranowski, M.; Serafin-Tkaczuk, M.; Magdziarz, A. Hydrothermal carbonization of agricultural and municipal solid waste digestates—Structure and energetic properties of the solid products. *Fuel* **2020**, *275*, 117837. [[CrossRef](#)]
20. Fang, J.; Zhan, L.; Ok, Y.S.; Gao, B. Minireview of potential applications of hydrochar derived from hydrothermal carbonization of biomass. *J. Ind. Eng. Chem.* **2018**, *57*, 15–21. [[CrossRef](#)]
21. Azzaz, A.A.; Khiari, B.; Jellali, S.; Ghimbeu, C.M.; Jeguirim, M. Hydrochars production, characterization and application for wastewater treatment: A review. *Renew. Sustain. Energy Rev.* **2020**, *127*, 109882. [[CrossRef](#)]
22. Wang, T.; Zhai, Y.; Zhu, Y.; Li, C.; Zeng, G. A review of the hydrothermal carbonization of biomass waste for hydrochar formation: Process conditions, fundamentals, and physicochemical properties. *Renew. Sustain. Energy Rev.* **2018**, *90*, 223–247. [[CrossRef](#)]
23. Tasca, A.L.; Puccini, M.; Gori, R.; Corsi, I.; Galletti, A.M.R.; Vitolo, S. Hydrothermal carbonization of sewage sludge: A critical analysis of process severity, hydrochar properties and environmental implications. *Waste Manag.* **2019**, *93*, 1–13. [[CrossRef](#)] [[PubMed](#)]

24. Zhai, Y.; Liu, X.; Zhu, Y.; Peng, C.; Wang, T.; Zhu, L.; Li, C.; Zeng, G. Hydrothermal carbonization of sewage sludge: The effect of feed-water pH on fate and risk of heavy metals in hydrochars. *Bioresour. Technol.* **2016**, *218*, 183–188. [[CrossRef](#)]
25. Werle, S.; Dudziak, M. Evaluation of toxicity of sewage sludge and gasification waste-products. *Przem. Chem.* **2013**, *92*, 1350–1353.
26. Shi, W.; Liu, C.; Ding, D.; Lei, Z.; Yang, Y.; Feng, C.; Zhang, Z. Immobilization of heavy metals in sewage sludge by using subcritical water technology. *Bioresour. Technol.* **2013**, *137*, 18–24. [[CrossRef](#)]
27. Berslin, D.; Reshmi, A.; Sivaprakash, B.; Rajamohan, N.; Kumar, P.S. Remediation of emerging metal pollutants using environment friendly biochar- Review on applications and mechanism. *Chemosphere* **2022**, *290*, 133384. [[CrossRef](#)]
28. Masoumi, S.; Borugadda, V.B.; Nanda, S.; Dalai, A.K. Hydrochar: A Review on Its Production Technologies and Applications. *Catalysts* **2021**, *11*, 939. [[CrossRef](#)]
29. Nandhini, R.; Berslin, D.; Sivaprakash, B.; Rajamohan, N.; Vo, D.V.N. Thermochemical conversion of municipal solid waste into energy and hydrogen: A review. *Environ. Chem. Lett.* **2022**, *20*, 1645–1669. [[CrossRef](#)]
30. Monisha, R.S.; Mani, R.L.; Sivaprakash, B.; Rajamohan, N.; Vo, D.V.N. Green remediation of pharmaceutical wastes using biochar: A review. *Environ. Chem. Lett.* **2022**, *20*, 681–704. [[CrossRef](#)]
31. Shi, W.; Liu, C.; Shu, Y.; Feng, C.; Lei, Z.; Zhang, Z. Synergistic Effect of rice husk addition on hydrothermal treatment of sewage sludge: Fate and environmental risk of heavy metals. *Bioresour. Technol.* **2013**, *149*, 496–502. [[CrossRef](#)] [[PubMed](#)]
32. Sharma, H.B.; Sarmah, A.K.; Dubey, B. Hydrothermal carbonization of renewable waste biomass for solid biofuel production: A discussion on process mechanism, the influence of process parameters, environmental performance and fuel properties of hydrochar. *Renew. Sustain. Energy Rev.* **2020**, *123*, 109761. [[CrossRef](#)]
33. Titirici, M.M.; Funke, A.; Kruse, A. Hydrothermal Carbonization of Biomass. In *Recent Advances in Thermo-Chemical Conversion of Biomass*; Elsevier: Amsterdam, The Netherlands, 2015; pp. 325–352.
34. Wilk, M.; Śliz, M.; Lubieniecki, B. Hydrothermal co-carbonization of sewage sludge and fuel additives: Combustion performance of hydrochar. *Renew. Energy* **2021**, *178*, 1046–1056. [[CrossRef](#)]
35. Gao, N.; Li, Z.; Quan, C.; Miskolczi, N.; Egedy, A. A new method combining hydrothermal carbonization and mechanical compression in-situ for sewage sludge dewatering: Bench-scale verification. *J. Anal. Appl. Pyrolysis* **2019**, *139*, 187–195. [[CrossRef](#)]
36. Breulmann, M.; van Afferden, M.; Müller, R.A.; Schulz, E.; Fühner, C. Process conditions of pyrolysis and hydrothermal carbonization affect the potential of sewage sludge for soil carbon sequestration and amelioration. *J. Anal. Appl. Pyrolysis* **2017**, *124*, 256–265. [[CrossRef](#)]
37. De la Rubia, M.A.; Villamil, J.A.; Rodriguez, J.J.; Mohedano, A.F. Effect of inoculum source and initial concentration on the anaerobic digestion of the liquid fraction from hydrothermal carbonisation of sewage sludge. *Renew. Energy* **2018**, *127*, 697–704. [[CrossRef](#)]
38. Wang, S.; Persson, H.; Yang, W.; Jönsson, P.G. Pyrolysis Study of hydrothermal carbonization-treated digested sewage sludge using a py-gc/ms and a bench-scale pyrolyzer. *Fuel* **2020**, *262*, 116335. [[CrossRef](#)]
39. Aragón-Briceño, C.; Ross, A.B.; Camargo-Valero, M.A. Evaluation and comparison of product yields and bio-methane potential in sewage digestate following hydrothermal treatment. *Appl. Energy* **2017**, *208*, 1357–1369. [[CrossRef](#)]
40. Parmar, K.R.; Ross, A.B. Integration of hydrothermal carbonisation with anaerobic digestion; opportunities for valorisation of digestate. *Energies* **2019**, *12*, 1586. [[CrossRef](#)]
41. Cao, Z.; Jung, D.; Olszewski, M.P.; Arauzo, P.J.; Kruse, A. Hydrothermal carbonization of biogas digestate: Effect of digestate origin and process conditions. *Waste Manag.* **2019**, *100*, 138–150. [[CrossRef](#)]
42. Werle, S. A reburning process using sewage sludge-derived syngas. *Chem. Pap.* **2012**, *66*, 99–107. [[CrossRef](#)]
43. Cao, Z.; Hülsemann, B.; Wüst, D.; Illi, L.; Oechsner, H.; Kruse, A. Valorization of maize silage digestate from two-stage anaerobic digestion by hydrothermal carbonization. *Energy Convers. Manag.* **2020**, *222*, 113218. [[CrossRef](#)]
44. Wilk, M. A Novel Method of Sewage Sludge Pre-Treatment-HTC. In Proceedings of the 1st International Conference on the Sustainable Energy and Environment Development (SEED 2016), Kraków, Poland, 17–19 May 2016; Volume 10.
45. Śliz, M.; Tuci, F.; Czerwińska, K.; Fabrizi, S.; Lombardi, L.; Wilk, M. Hydrothermal carbonization of the wet fraction from mixed municipal solid waste: Hydrochar characteristics and energy balance. *Waste Manag.* **2022**, *151*, 39–48. [[CrossRef](#)] [[PubMed](#)]
46. Ozawa, T. Estimation of activation energy by isoconversion methods. *Thermochim. Acta* **1992**, *203*, 159–165. [[CrossRef](#)]
47. He, C.; Giannis, A.; Wang, J.Y. Conversion of sewage sludge to clean solid fuel using hydrothermal carbonization: Hydrochar fuel characteristics and combustion behavior. *Appl. Energy* **2013**, *111*, 257–266. [[CrossRef](#)]
48. Song, C.-Z.; Wen, J.-H.; Li, Y.-Y.; Dan, H.; Shi, X.-Y.; Xin, S. Thermogravimetric assessment of combustion characteristics of blends of lignite coals with coal gangue. In Proceedings of the 3rd Annual International Conference on Mechanics and Mechanical Engineering (MME 2016), Chengdu, China, 16–18 December 2016; Volume 105, pp. 490–495.
49. Magdziarz, A.; Wilk, M.; Straka, R. Combustion Process of torrefied wood biomass: A kinetic study. *J. Therm. Anal. Calorim.* **2017**, *127*, 1339–1349. [[CrossRef](#)]
50. Barzegar, R.; Yozgatligil, A.; Olgun, H.; Atimtay, A.T. TGA and kinetic study of different torrefaction conditions of wood biomass under air and oxy-fuel combustion atmospheres. *J. Energy Inst.* **2020**, *93*, 889–898. [[CrossRef](#)]
51. Ren, S.; Lei, H.; Wang, L.; Bu, Q.; Chen, S.; Wu, J. Thermal Behaviour and kinetic study for woody biomass torrefaction and torrefied biomass pyrolysis by TGA. *Biosyst. Eng.* **2013**, *116*, 420–426. [[CrossRef](#)]

52. Peng, C.; Zhai, Y.; Zhu, Y.; Xu, B.; Wang, T.; Li, C.; Zeng, G. Production of char from sewage sludge employing hydrothermal carbonization: Char properties, combustion behavior and thermal characteristics. *Fuel* **2016**, *176*, 110–118. [[CrossRef](#)]
53. Zheng, X.; Jiang, Z.; Ying, Z.; Song, J.; Chen, W.; Wang, B. Role of feedstock properties and hydrothermal carbonization conditions on fuel properties of sewage sludge-derived hydrochar using multiple linear regression technique. *Fuel* **2020**, *271*, 117609.
54. Lin, Y.; Wang, D.; Wang, T. Ethanol Production from pulp & paper sludge and monosodium glutamate waste liquor by simultaneous saccharification and fermentation in batch condition. *Chem. Eng. J.* **2012**, *191*, 31–37.
55. Zhuang, X.; Zhan, H.; Song, Y.; He, C.; Huang, Y.; Yin, X.; Wu, C. Insights into the evolution of chemical structures in lignocellulose and non-lignocellulose biowastes during hydrothermal carbonization (HTC). *Fuel* **2019**, *236*, 960–974. [[CrossRef](#)]
56. Wang, L.; Chang, Y.; Li, A. Hydrothermal carbonization for energy-efficient processing of sewage sludge: A review. *Renew. Sustain. Energy Rev.* **2019**, *108*, 423–440. [[CrossRef](#)]